Experimental test of model for angular and energy dependence of reflection-electron-energy-loss spectra

F. Yubero,* D. Fujita,† B. Ramskov, and S. Tougaard
Department of Physics, Odense University, DK-5230 Odense M, Denmark
(Received 14 August 1995)

Experimental inelastic electron-scattering cross sections of Si and Fe determined from reflection-electron-energy-loss spectroscopy (REELS) experiments are presented. Three primary energies of the electrons (300, 800, and 2000 eV) and three experimental geometries have been considered. The cross sections have been compared with those determined according to a theoretical model introduced in the preceding paper [F. Yubero *et al.*, Phys. Rev. B **53**, 9719 (1996)]. The agreement between theory and experiment is good, considering that the theoretical cross sections are calculated from first principles, without adjustable parameters. For a fixed primary electron energy the inelastic mean free path, for both Si and Fe, is found to decrease for more glancing trajectories. The characteristic length for the path-length distribution function of the REELS electrons is found to be smaller for Fe than for Si and to decrease with energy for both materials.

I. INTRODUCTION

In Ref. 1, a model was described to calculate the inelastic scattering cross section for electrons traveling in a general reflection-electron-energy-loss-spectroscopy (REELS) geometry. In this paper we want to test the validity of that model by comparing the theoretical predictions with experimentally determined inelastic electron scattering cross sections $K(E_0,\hbar\omega)$.

In the past, different models have been used to interpret experimental REELS data.[1–10] After Tougaard and Chorkendorff[7] introduced the formalism to obtain $K(E_0,\hbar\omega)$ from measured REELS experiments, several attempts have been done to reproduce it theoretically, from first principles calculations.[8–10]

Tougaard and Kraaer[8] presented a systematic study. They calculated inelastic electron scattering cross sections from measured REELS experiments of several materials and primary electron energies. They were interested in the dependence of $K(E_0,\hbar\omega)$ on the primary energy E_0, and therefore they used a geometry with incidence and exit angles close to the surface normal to minimize surface excitations. Besides, they calculated theoretical inelastic electron scattering cross sections for the materials assuming that the electrons were traveling in an infinite medium. The dielectric function ϵ of the medium was the only input in their calculations. For very large E_0 (several thousands of eV) they found good agreement between theory and experiment. However, at lower energies, surface excitations were found to be important and the agreement was bad.

Some years later Yubero and Tougaard[9] made a theoretical model for REELS based on first principles. They considered a geometry with normal incidence and exit angles for the primary electrons and again ϵ was the only input in the calculations. This model takes into account bulk and surface contributions, the interference effects between the field set up by the incidence electron on the reflected electron and the path-length distribution of the electrons contributing to $K(E_0,\hbar\omega)$. Theoretical calculations of the inelastic electron scattering cross section obtained with this model were compared with the previous experimental $K(E_0,\hbar\omega)$ obtained by Tougaard and Kraaer.[8] It was found that the general trends of the loss features appearing in the experimental cross sections as the primary energy was changed were well reproduced by the theory.

Recently, Tung *et al.*[10] have considered another model to reproduce experimental $K(E_0,\hbar\omega)$. They obtain very good agreement with $K(E_0,\hbar\omega)$ determined experimentally.[8] The validity of their model has been briefly discussed in the preceding paper.[1]

The presently used model is based on the so-called ''surface reflection model''.[11] It allows one to include the geometry as well as the energy dependence of inelastic electron scattering cross section as measured from REELS experiments. It is worth mentioning that model B in Ref. 9, which has been applied successfully to the determination of optical properties of several materials,[12,13] appears as a particular case for a given geometry (incidence and exit angles normal to the surface) of the formalism in Ref. 1.

In the following we describe briefly the method to obtain both experimental and theoretical inelastic electron scattering cross sections and we discuss the results of the quantitative study of the analysis of the spectra.

II. EXPERIMENT

REELS spectra were measured with a commercial electron spectrometer (VG-CLAM100) equipped with a hemispherical electron-energy analyzer, an electron gun, a dual x-ray source, and an ion gun. The angle between the input lens of the analyzer and the electron gun was 25°. To measure at different experimental geometries, three types of special sample holders were designed to specify the angles for incident θ_i and exit electrons θ_o to be $(\theta_i,\theta_o)=(0°,25°)$, $(50°,-25°)$, and $(75°,-50°)$ (see Fig. 1). The polycrystalline Fe (99.9%) and Si (99.999%, *n*-type) specimens were cut and mounted in a vacuum chamber with a base pressure of about 10^{-10} Torr. Their surfaces were cleaned and disordered by prolonged ion bombardment with 2-keV Ar^+. The surface

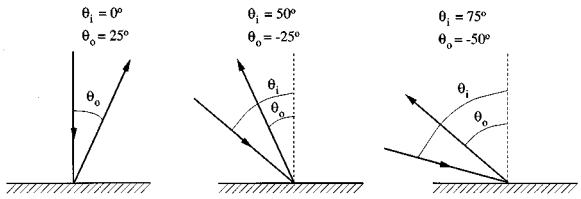

FIG. 1. Geometries used for the REELS experiments.

cleanliness was frequently checked by Auger electron spectroscopy, and only samples with a surface contamination below ~1% with respect to any contamination were considered acceptable.

The measurement conditions for REELS were as follows. For the incident electron beam, three primary energy E_0 of 300, 800, and 2000 eV were used. Spectra were measured at FAT (fixed analyzer transmission) mode with the pass energy of 50 eV, which corresponds to an absolute energy resolution of ~1 eV. Because of the large difference in intensity, the elastic peak and its tail region (up to 150 eV below E_0) were recorded separately and recombined together afterwards to make a single spectrum (see description in Ref. 8). Then, the measured spectra were corrected for the energy dependence of the analyzer transmission function determined by calibration against the NPL (National Physical Laboratory) metrology spectrometer.[14]

III. EXPERIMENTAL CROSS SECTIONS

An experimental REELS spectrum $j_l(E)$ has contributions from both single and multiple inelastically scattered electrons. We can remove the multiple-scattering contribution and determine $K(E_0,\hbar\omega)$ by the algorithm[7]

$$\frac{\lambda L}{\lambda+L}K(E_0,E_0-E)=\frac{1}{c}\left[j_l(E)-\int_E^{E_0}\frac{\lambda L}{\lambda+L}K(E_0,E'-E)j_l(E')dE'\right], \quad (1)$$

where λ is the inelastic mean free path, L is the attenuation length for the path-length distribution of the reflected electrons due to the effect of the elastic scattering, $\hbar\omega=E_0-E$ is the energy loss by the primary electrons, and c is the elastic peak area. The prefactor $L/(L+\lambda)$ in Eq. (1) can be obtained by the condition

$$\int_0^{\infty}\frac{\lambda L}{\lambda+L}K(E_0,\hbar\omega)d\hbar\omega=\frac{L}{\lambda+L}. \quad (2)$$

In our case energy losses $\hbar\omega$ up to 150 eV were measured, which is large enough to make a good estimate of the total area of $K(E_0,\hbar\omega)$. Finally $K(E_0,\hbar\omega)$ will be determined taking λ either from the literature or from the inverse of the area of theoretically determined cross sections.

The validity of Eq. (1) for the determination of $K(E_0,\hbar\omega)$ has been discussed before.[7,8] It is expected to give realistic results for $\hbar\omega<\hbar\omega_s+\hbar\omega_p$ where $\hbar\omega_s$ and $\hbar\omega_p$ are, respectively, the surface and bulk plasmon energies of the solid.[7] For $\hbar\omega>\hbar\omega_s+\hbar\omega_p$ it is expected that the real value of $K(E_0,\hbar\omega)$ is underestimated. This is due to the different behavior of the surface losses with respect to the bulk losses that is not taken into account in the derivation of

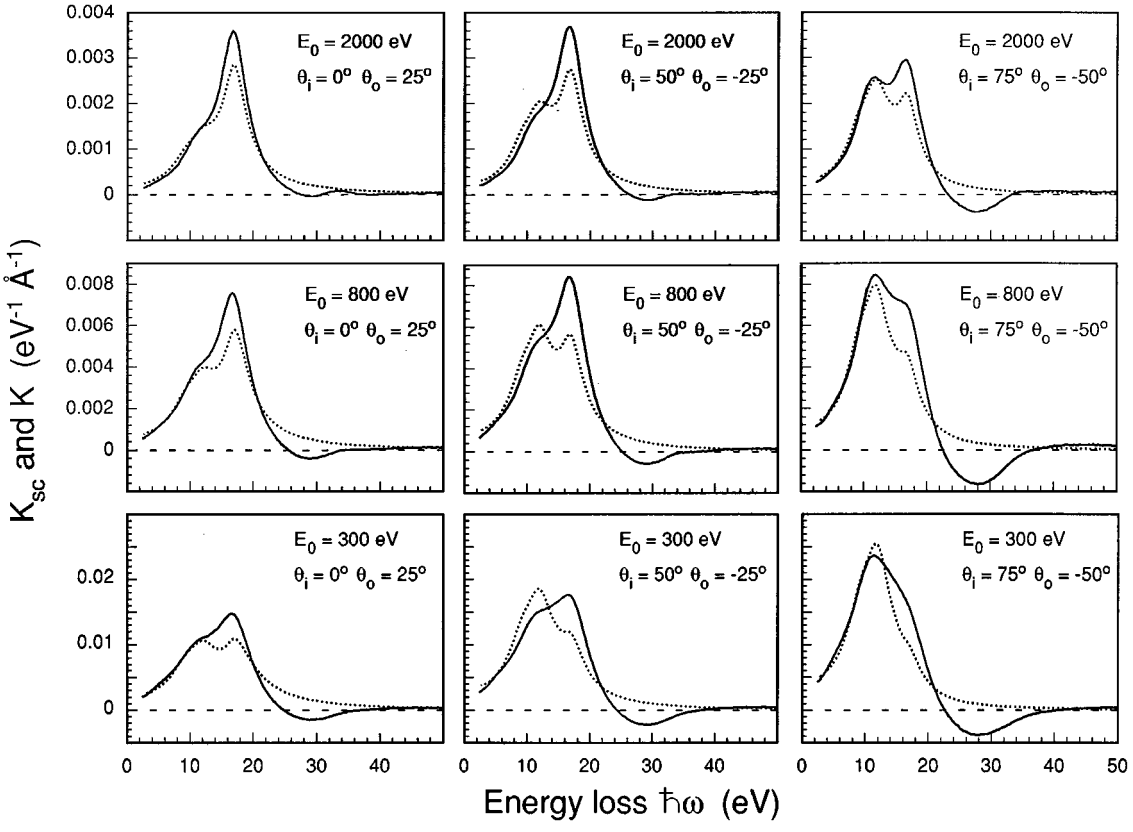

FIG. 2. Inelastic electron scattering cross sections for Si calculated from experiments (full lines) and from the present theory (points).

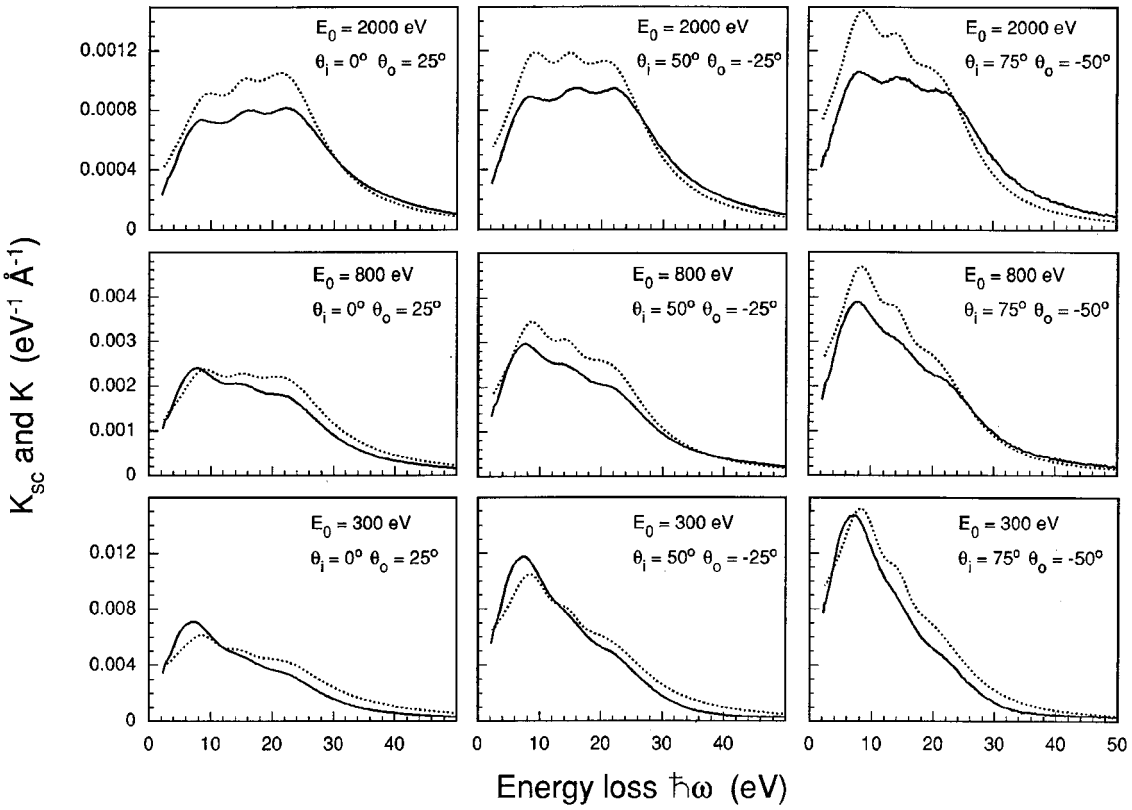

FIG. 3. Inelastic electron scattering cross sections for Fe calculated from experiments (full lines) and from the present theory (points).

Eq. (1). This effect is clearly observed for Al and Si, for which surface and bulk losses are clearly separated,[7,8] but is less obvious for other materials with broad loss functions.

IV. THEORETICAL CROSS SECTIONS AND INELASTIC MEAN FREE PATHS

In Ref. 1, a theory was presented that allows one to calculate the inelastic electron scattering cross section $K_{sc}(E_0,\hbar\omega,\theta_i,\theta_o)$ as a function of the dielectric function ϵ, the electron energy E_0, and the experimental geometry (θ_i and θ_o are the incidence and exit angles for the electrons with respect to the surface normal).

For a given $K_{sc}(E_0,\hbar\omega,\theta_i,\theta_o)$, the theoretical inelastic mean free path $\lambda_{sc}(E_0,\theta_i,\theta_o)$ is defined as

$$[\lambda_{sc}(E_0,\theta_i,\theta_o)]^{-1}=\int_0^{E_{max}} d\hbar\omega K_{sc}(E_0,\hbar\omega,\theta_i,\theta_o) + [\lambda_c(E_0)]^{-1}, \quad (3)$$

where E_{max} is the maximum energy $\hbar\omega$ available for K_{sc} and λ_c accounts for the scattering contribution of the core levels at binding energies above E_{max}.[15]

V. RESULTS AND DISCUSSION

The inelastic scattering cross sections $K(E_0,\hbar\omega)$ obtained from experimental data by applying the procedure described in the experimental section are depicted as full lines in Fig. 2 for Si and in Fig. 3 for Fe. Three primary energies (E_0=300, 800, and 2000 eV) and three geometries for incident and exit electrons [(θ_i,θ_o)=(0°,25°), (50°,−25°), and (75°,−50°), see Fig. 1] are considered. Besides, these figures include the corresponding theoretical calculations of $K_{ac}(E_0,\hbar\omega,\theta_i,\theta_o)$ (points) according to Eq. (26) in the previous paper.[1] The dielectric functions for Si and Fe were taken from Ref. 12 and Ref. 8, respectively. The attenuation length L was taken to be ∞ for all the theoretical calculations for simplicity. Below we discuss the validity of this approximation.

The qualitative agreement between theory and experiment

TABLE I. $L/(L+\lambda)$ from Eq. (2) for Si for the primary energies and geometries considered.

Si	E_0 (eV)		
(θ_i,θ_0)	300	800	2000
(0,25)	0.979	0.971	0.986
(50,−25)	0.964	0.977	0.989
(75,−50)	0.967	0.957	0.961

TABLE II. $L/(L+\lambda)$ from Eq. (2) for Fe for the primary energies and geometries considered.

Fe	E_0 (eV)		
(θ_i,θ_0)	300	800	2000
(0,25)	0.886	0.848	0.947
(50,−25)	0.861	0.897	0.959
(75,−50)	0.922	0.895	0.948

TABLE III. Theoretical inelastic electron mean free paths $\lambda_{sc}(E_0,\theta_i,\theta_o)$ (in Å) calculated from Eq. (3), for the primary energies and geometries considered for Si. The inelastic mean free path from Ref. 18 (λ_{TPP2}) are included for comparison.

Si	E_0 (eV)		
(θ_i,θ_0)	300	800	2000
(0,0)	8.3	18.0	39.6
(0,25)	5.3	13.1	31.1
(50,−25)	4.3	11.4	28.8
(75,−50)	3.8	11.0	30.1
λ_{TPP2}	10.3	20.6	42.5

for both Si (Fig. 2) and Fe (Fig. 3) is good. As the primary energy increases, the relative importance of surface excitations decreases. Besides, the relative importance of surface excitations increases as the geometry gets more glancing. These effects are observed for both theory and experiment for each geometry and energy considered.

For Si in Fig. 2, surface and bulk plasmons are clearly identified as the features at ~11 and ~17 eV, respectively. The negative excursion of the experimental cross sections at ~28 eV has been discussed above. It appears at $\sim\hbar\omega_s+\hbar\omega_p$ and is due to the deficiencies of the algorithm to subtract the multiple scattering from an experimental REELS experiment.[7] That is why the negative excursion gets more pronounced when surface excitations are enhanced, i.e., for lower primary energies and more glancing geometries.

Notice that for Si in Fig. 2, both theory and experiment show more surface losses for the more glancing geometry [i.e., $(\theta_i,\theta_o)=(75°,-50°)$] at 2000 eV than the more normal geometry [i.e., $(\theta_i,\theta_o)=(0°,25°)$] at 300 eV. However, for Fe in Fig. 3, this is not the case.

Not only the shape but also the absolute values of the theoretical cross sections are close to the experimentally determined cross sections. However, for Si the bulk plasmon peak is underestimated by theory. Note that the theoretical cross sections are calculated from first principles, the only input in the calculations is the dielectric function and no adjustable parameters have been applied.

Tables I and II show, for Si and Fe, the experimental values of the quantity $L/(L+\lambda)$ obtained from Eq. (2). The obtained values are close to unity as expected since in general $L \gg \lambda$.[7,8]

TABLE IV. Theoretical inelastic electron mean free paths $\lambda_{sc}(E_0,\theta_i,\theta_o)$ (in Å) calculated from Eq. (3), for the primary energies and geometries considered for Fe. The inelastic mean free path from Ref. 18 (λ_{TPP2}) are included for comparison.

Fe	E_0 (eV)		
(θ_i,θ_o)	300	800	2000
(0,0)	7.9	16.9	35.9
(0,25)	5.4	12.3	28.4
(50,−25)	4.0	10.4	25.8
(75,−50)	3.3	9.3	25.1
λ_{TPP2}	7.2	13.7	27.7

TABLE V. Attenuation length L (in Å) obtained from Eq. (4) for Si for the primary energies and geometries considered.

Si	E_0 (eV)		
(θ_i,θ_o)	300	800	2000
(0,25)	250	440	2200
(50,−25)	120	480	2600
(75,−50)	110	250	740

The obtained values for the theoretical inelastic electron mean free paths $\lambda_{sc}(E_0,\theta_i,\theta_o)$ calculated from Eq. (3), for the primary energies and geometries considered, are shown in Table III for Si and in Table IV for Fe. Besides, inelastic mean free path from Ref. 18 (λ_{TPP2}) are included for comparison. Note that most of the values for λ_{sc} are smaller than those of Tanuma, Powell, and Penn.[18] This is primarily because our model includes the effect of the energy loss of the electrons as they travel in vacuum close to the surface. The path length over which the electron can interact with the solid while it is above the surface increases for the more glancing geometries. This results in a decreasing inelastic mean free path for glancing trajectories as observed in Tables III and IV. Note that the dependency of λ_{sc} on geometry is stronger for lower primary energies and is more pronounced for Fe than for Si.

We can estimate the attenuation length,

$$L=\frac{\lambda_{sc}}{(L/(L+\lambda))^{-1}-1}, \tag{4}$$

where $L/(L+\lambda)$ is taken from Tables I and II, and λ_{sc} is taken from Tables III and IV. The thus obtained values for L are shown in Table V for Si and in Table VI for Fe. We observe that L is smaller for Fe than for Si at the corresponding energies and geometries. Furthermore, L is smaller at lower energies. This behavior is to be expected, because the elastic scattering cross section is larger for heavier elements and for lower energies.[16,17]

The discrepancies observed between theory and experiment could be due to the following effects:

(1) The dielectric function, and in particular the assumed dependence on momentum transfer, might be inaccurate. Recently a new parametrization of the dielectric function was proposed[19] for Fe where special care is taken in the fulfill-

TABLE VI. Attenuation length L (in Å) obtained from Eq. (4) for Fe for the primary energies and geometries considered.

Fe	E_0 (eV)		
(θ_i,θ_o)	300	800	2000
(0,25)	42	69	510
(50,−25)	25	91	600
(75,−50)	39	79	460

ment of sum rules for the dielectric function that might improve the match between theory and experiment.

(2) Additionally, as the values of L in Tables V and VI show, all path lengths are not equally probable as is assumed in the theoretical calculations [Eq. (26) in Ref. 1]. Including this effect would change the relative importance of surface excitations for small values of L/λ, although considering the large values of L in Tables V and VI, we expect the effect to be quite small.

(3) Furthermore, in the theoretical model it is assumed that the electrons experience only a single elastic large-angle scattering event. This approximation is expected to be reasonable since small-angle scattering, which is the most probable, would not affect the validity of the present theory. However, the contributions from backscattered electrons that have undergone two or more large-angle scattering events might be a source of error.

VI. CONCLUSIONS

Experimental inelastic scattering cross sections of Si and Fe determined at primary energies of 300, 800, and 2000 eV at different geometries have been presented. They have been compared with those determined according to a theoretical model introduced in Ref. 1. Good quantitative agreement is found between the theoretical predictions and the experimental findings for the inelastic scattering cross sections. The theoretically calculated inelastic mean free path is found to depend on both energy and geometry. For a fixed energy, the inelastic mean free path is smaller for glancing trajectories.

Besides, the characteristic length for the path-length distribution function of the REELS electrons is estimated. It is found to be smaller for Fe than for Si and to decrease with energy for both materials.

*Permanent address: LURE, Bât. 209d, Centre Universitaire Paris-Sud, F-91405 Orsay, France.

†Permanent address: National Research Institute for Metals, Tsukuba 305, Japan.

[1] F. Yubero, J. M. Sanz, B. Ramskov, and S. Tougaard, preceding paper, Phys. Rev. B **53**, 9719 (1996).

[2] G. Chiarello, E. Colavita, M. De Crescenzi, and S. Nannarone, Phys. Rev. B **29**, 4878 (1984).

[3] Y. Ohno, Phys. Rev. B **36**, 7500 (1987); **39**, 8209 (1989).

[4] J. C. Ingram, K. W. Nebesny, and J. E. Pemberton, Appl. Surf. Sci. **44**, 279 (1990); **44**, 293 (1990); **45**, 247 (1990).

[5] F. Yubero, J. M. Sanz, E. Elizalde, and L. Galán, Surf. Sci. **237**, 173 (1990); **251/252**, 296 (1991).

[6] G. Mondio, F. Neri, S. Patane, A. Arena, G. Marletta, and F. Iacona, Thin Solid Films **207**, 313 (1992).

[7] S. Tougaard and I. Chorkendorff, Phys. Rev. B **35**, 6570 (1987).

[8] S. Tougaard and J. Kraaer, Phys. Rev. B **43**, 1651 (1991).

[9] F. Yubero and S. Tougaard, Phys. Rev. B **46**, 2486 (1992).

[10] C. J. Tung, Y. F. Chen, C. M. Kwei, and T. L. Chou, Phys. Rev. B **49**, 16 684 (1994).

[11] R. H. Ritchie and A. L. Marusak, Surf. Sci. **4**, 234 (1966); J. L. Gervasoni and N. R. Arista, *ibid.* **260**, 329 (1992).

[12] F. Yubero, S. Tougaard, E. Elizalde, and J. M. Sanz, Surf. Interface Anal. **20**, 719 (1993).

[13] F. Yubero, J. M. Sanz, J. F. Trigo, E. Elizalde, and S. Tougaard, Surf. Interface Anal. **22**, 124 (1994).

[14] M. P. Seah, Surf. Interface Anal. **20**, 243 (1993).

[15] D. R. Penn, J. Electron Spectrosc. Relat. Phenom. **9**, 29 (1976).

[16] M. E. Riley, C. J. MacCallum, and F. Biggs, At. Data Nucl. Data Tables **15**, 443 (1975); **28**, 379 (1983).

[17] A. Jablonski, Surf. Interface Anal. **14**, 659 (1989).

[18] S. Tanuma, C. J. Powell, and D. R. Penn, Interface Anal. **17**, 911 (1991).

[19] C. M. Kwei, Y. F. Chen, C. J. Tung, and J. P. Wang, Surf. Sci. **293**, 202 (1993).